

Article

Thermal Environment Prediction for Metro Station base on RVFL Neural Network

Tian Qing¹, Zhao Weihang¹, Wei Yun², Pang Liping³

¹ North China University of Technology, Beijing, China, tianqing@ncut.edu.cn, zwh140410@163.com

² Beijing Urban Construction Design & Development Group Co., Ltd., Beijing, China, luckyboy0309@163.com

³ Beijing University of Aeronautics and Astronautics, Beijing, China; pangliping@buaa.edu.cn

Received: date; Accepted: date; Published: date

Abstract: With the improvement of China's metro carrying capacity, people in big cities are inclined to travel by metro. The carrying load of these metros is huge during the morning and evening rush hour. Coupled with the increase of summer tourists, the thermal environmental quality in early metro stations will decline badly. Therefore, it is necessary to analyze the factors that affect the thermal environment in the metro station and establish a thermal environment change model. This will help to support the prediction and analysis of the thermal environment in such limited underground spaces. In order to achieve a relatively accurate and rapid on-line modeling, this paper proposes a thermal environment modeling method based on Random Vector Functional Link Neural Network (RVFLNN). This modeling method has the advantages of fast modeling speed and relatively accurate prediction results. Once the preprocessed data is input into this RVFLNN for training, the metro station thermal environment model will be quickly established. The study results show that the thermal model based on the RVFLNN method can effectively predict the temperature inside the metro station.

Keywords: RVFLNN; thermal environment; temperature prediction; metro station

1. Introduction

There are two common methods to establish a thermal model in a space: the distributed parameter method and the lumped parameter method. The distribution parameter model is usually established by numerical approximation and discretization using the finite element method. Literatures¹⁻² use the distribution parameter method to establish heat transfer model, and achieve the distribution and prediction of object temperature. However, this method has the disadvantages of high computational cost and slow solution process. The lumped parameter model is established for the thermal node network method. The method uses the lumped parameter idea, which equates the object to a thermal node with uniform internal properties. Because of its simple principle, this method has been widely used in the field of heat transfer modeling³⁻⁶. One branch in lumped parameter method is neural network method. In recent years, with the development of artificial intelligence technology, the Artificial Neural Network (ANN) method gains more and more attention of scholars. The ANN possesses the advantage of strong non-linear fitting ability. It has become the main research direction to build the heat transfer model. This modeling technology does not require much knowledge about process mechanics and it just uses enough experimental data⁷⁻¹¹. Recently, the ANN method has been used to establish the nonlinear heat transfer model and predict

the temperature trend. This method avoids the difficulty of developing accurate models due to complex thermal processes¹²⁻¹³. The authors proposed the use of cellular neural networks and the Tree-Structure Ensemble General Regression Neural Networks (TSE-GRNNs) to establish heat transfer model. However, the ANN training process with a back-propagation algorithm has the disadvantage of slow convergence and long learning time. In contrast, the RVFLNN can overcome these shortcomings. The RVFLNN can fit any non-linear function by a linear combination of basis function, randomly assign input weights and bias¹⁴. It uses the least-square method to train its output weights¹⁵. The training process does not require iteration. Hence, it has a great advantage over the traditional ANN in terms of learning speed¹⁶.

This paper aims at using the RVFLNN to quickly establish the thermal environment model for a metro station. This presented modeling method tries to predict the change trend of temperature accurately inside the metro station. The RVFL network prediction model is obtained by analyzing the measured data at specified points from a metro station. The data for the input layer include temperatures, the passenger flow and the arrival frequency of metro vehicle. Finally, relatively good prediction results for the metro station can be obtained using the presented the thermal prediction method based on the RVFLNN.

2. Training principle of RVFLNN model

The RVFLNN has a good ability to fast model a nonlinear process. Its basic structure is shown in Fig. 1¹⁷.

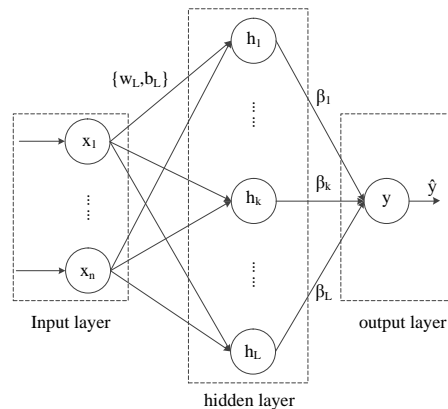


Fig. 1 RVFLNN structure

(1) Input layer: $X_{d,N} \in R^{d \times N}$ is a give training set and it is a $d \times N$ dimensional vector. W_L and B_L are weights and biases from the input layer to the hidden layer. $W_L \in R^L$ and $B_L \in R^L$. Here, d , N and L are the dimension of input variables, the number of samples and the number of hidden layer nodes, respectively. W_L and B_L are chosen in the beginning of the learning process, independently of the training data. In particular, W_L and B_L are chosen randomly from a predefined probability distribution in a RVFLNN. Hence, the input sets, weights and biases of RVFLNN are given by:

$$X_{d,N} = \begin{pmatrix} x_{1,1} & \cdots & x_{1,N} \\ \vdots & \ddots & \vdots \\ x_{d,1} & \cdots & x_{d,N} \end{pmatrix} \quad (1a)$$

$$W_L = (w_1, \dots, w_L), \quad B_L = (b_1, \dots, b_L) \quad (1b)$$

(2) Hidden layer: The purpose of the hidden layer is to establish an activation function, $H_{L,N}$, for the hidden layer node. From Eq. (2), each h_l is a fixed non-linear function known as hidden function. In our paper, the sigmoid basis function is given by:

$$h_l = \frac{1}{1 + \exp(-w_l^T x_i + b_l)} \quad (2)$$

Finally, the hidden matrix, $H_{N,L}$, is denoted by Eq. (3):

$$H_{N,L} = \begin{pmatrix} h_{1,1} & \cdots & h_{1,L} \\ \vdots & \ddots & \vdots \\ h_{N,1} & \cdots & h_{N,L} \end{pmatrix} \quad (3)$$

(3) Output layer: A desired output, $Y_N = (y_1, \dots, y_j, \dots, y_N)'$, is a N dimensional vector. The output of an RVFLNN can be described as:

$$f(x) = \sum_{l=1}^L \beta_l h_l \quad (4)$$

Therefore, Eq. (4) can be expressed in the form of matrix:

$$Y_N = H_N \beta \quad (5)$$

The output weights, $\beta_L = (\beta_1, \dots, \beta_l, \dots, \beta_L)$, is the purpose of training, so the learning problem can be formulated as minimizing both the training error and the output weight norm:

$$\min_{\beta} \frac{1}{2} \|H_{N,L} \beta_L - Y_N\|_2^2 + \frac{\lambda}{2} \|\beta_L\|_2^2, \lambda > 0 \quad (6)$$

where the factor $\frac{1}{2}$ is added for successive simplifications; λ is the complexity coefficient. We

obtain the well-known solution for β_L :

$$\beta_L = (H_{N,L}^T H_{N,L} + \lambda I)^{-1} H_{N,L}^T Y_N$$

where I is the identity matrix of proper dimensions to prevent numerical instabilities. Thus the learning process can be completed using Eq.(1) ~ Eq.(7).

3. Measurement process

3.1 Test points in metro station

The measured metro station is an early station. Passengers can go down to the metro station from the upper platform by three stairs. The measured temperature points were distributed at four locations, S1, S2, S3 and S4, respectively. S1 was at the upper platform and its temperature was very similar to the air supply temperature of air conditioning system. S2, S3 and S4 were at the lower platform. Point R was the passenger flow monitoring point.

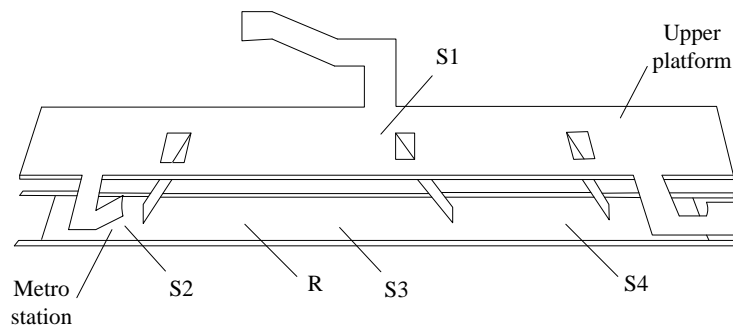


Fig. 1 Metro station measuring point distribution.

3.2 Data acquisition and processing

(1) The temperatures were monitored for 3 days and recorded every 2 minutes for a total of 2160 data points. T_1 , T_2 , T_3 and T_4 are temperatures at S1, S2, S3 and S4, respectively, as shown in the Fig.2. They are processed from the row data with a Butterworth filter. The first 720 data points were measured on Sunday, the second 720 data and the third 720 data points were measured on Monday and Tuesday, respectively.

(2) Passenger flow monitoring point was at Point R. The number of passengers, P_{flow} , was monitored every two minutes. Fig. 3 is the passenger flow curve after been processed with median filtering. It is very obvious that the passenger flow data is very different between weekdays and weekends.

(3) Since the metro arrival frequency, F_{train} , varies significantly with the time and the number of passengers, Fig. 4 gives the change of F_{train} with time. It can be seen that F_{train} is obviously changed with the morning and evening rush hour. F_{train} is also different for weekdays and weekends.

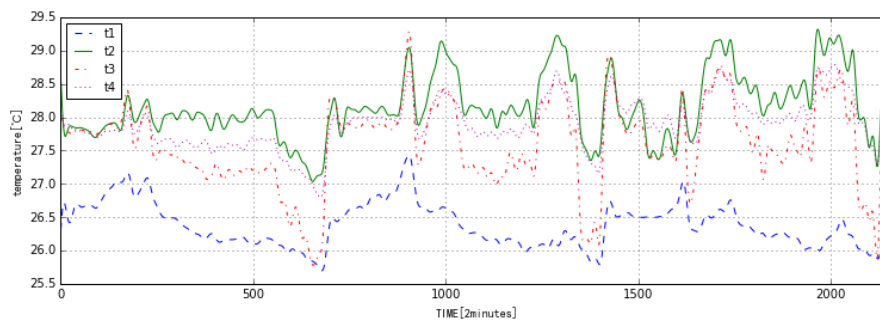
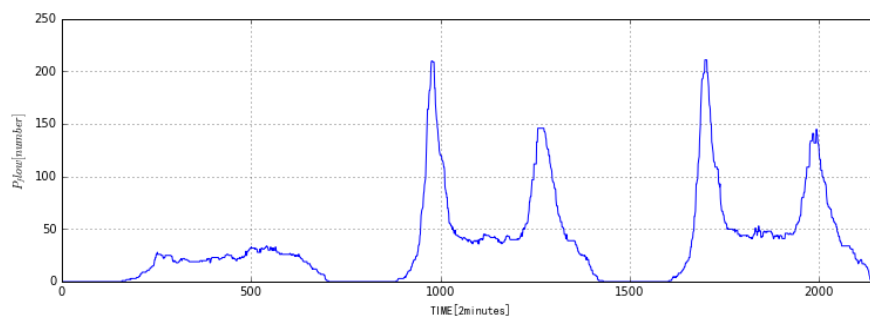
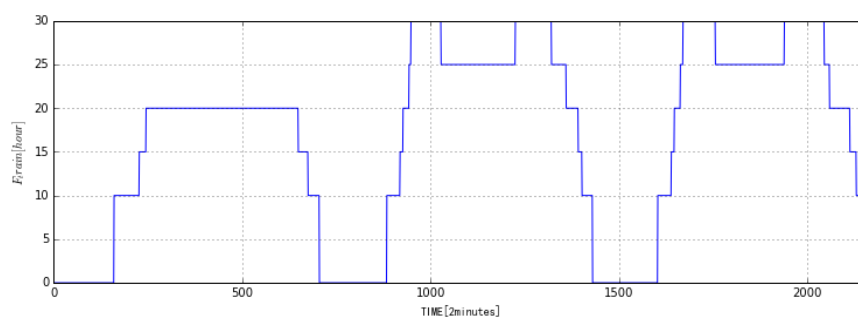
**Fig. 2** processed temperature data.**Fig. 3** processed passenger flow data.

Fig. 4 metro train arrival frequency.



3.3 Thermal environment model based on RVFLNN for metro station

3.3.1 Model input and output

In fact, there are many parameters that will influence the climate, such as the air velocity, the relative humidity, the diffused thermal radiation and the latent thermal load due to the presence of people. Because of the limitations of our measuring instruments, only the parameters of temperature and relative humidity at S1, S2, S3 and S4 were measured. In later analysis, we found the relative humidity did not fluctuate greatly and remained within a certain range, hence the relative humidity and temperature were not so correlated. The relative humidity doesn't use to predict the temperature. In addition, the airflow velocity in the subway station is related to the frequency of the subway train, and the radiation is related to the number of passengers. Therefore, our temperature prediction is finally based on the temperatures in different places, passengers flow, and metro arrival frequency.



Because of the structure of the entire metro station, the air from S1 can bring cool wind to the downstairs and directly affect the temperature of S2, S3 and S4. At the same time, whenever the metro train arrives, the air flow change and the passenger flow all influence the temperature of S2, S3 and S4. The temperature of S1 affects the ones of S2, S3 and S4. But S2, S3 and S4 influence each other. The whole space in the metro station is divided in three sub-spaces, S2, S3 and S4. In this paper, the thermal models will be built for S2, S3 and S4 in the metro station, separately. For sub-space S2, its parameters of input layer are determined as T_1 , T_3 , P_{flow} and F_{train} . For sub-space S3, its parameters of input layer are determined as T_1 , T_2 , T_4 , P_{flow} and F_{train} . For sub-space S4, its parameters of input layer are determined as T_1 , T_3 , P_{flow} and F_{train} . So T_1 , P_{flow} and F_{train} will be the common training input variables for S2, S3 and S4. The final structures of traditional RVFL for temperature models of T_2 , T_3 and T_4 are shown in Fig. 5. The temperature prediction accuracy of S2 to S4 can be improved by establishing different neural network models.

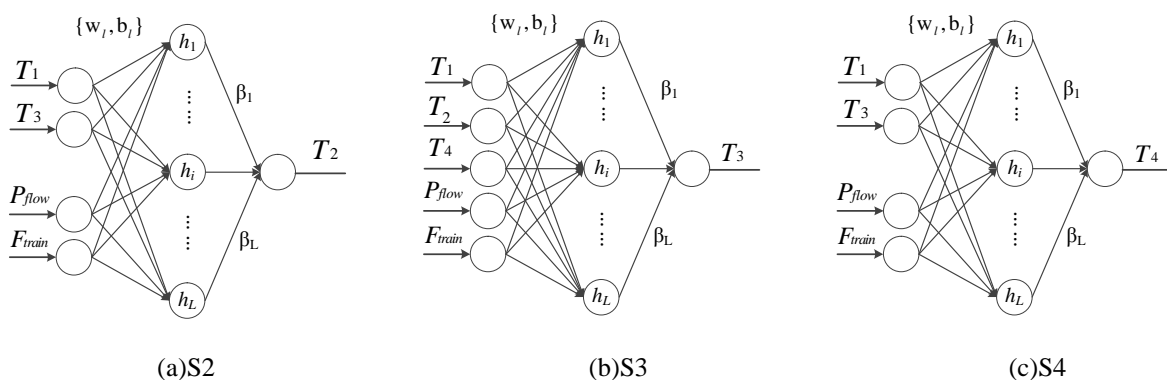


Fig. 5 Final structures of traditional RVFL.

Because the data were measured in three days, Sunday, Monday and Tuesday, the passenger flow and the metro arrival frequency are very different between weekdays and weekends. In order to obtain better prediction performance, the data of the first two days are used for the training. The data of the last day are as the test data.



3.3.2 Input normalization



The input data is normalized with Eq. (8).

$$x' = \frac{x - x_{\min}}{x_{\max} - x_{\min}} \quad (8)$$

where x' denotes normalized data; x is the filtered data; x_{\min} is the minimum value of x ; x_{\max} is the maximum value of x .

The meaning of normalization is making the input variables with different physical dimensions equal to be used. In the meantime, the sigmoid function is used as a transfer function in the RVFLNN. The normalization can prevent the neuron output saturation caused by excessive absolute value of net input.

3.3.3 Build the model

We have established three neural network models. Every neural network step is the same.

The processes are as following steps:

Step 1: Divide training set, validation set and test set

The data were measured in three days, Sunday, Monday and Tuesday. A total number of sample points is 2160. We use the first 1440 sample points as the training set, the next 360 sample points as validation set and the last 360 sample points as the test set.

Step 2: Set the number of neural network nodes

From Fig. 5, the input layer consists of 4, 5 and 4 neurons for T_2 , T_3 and T_4 , separately. The output layer has 1 neuron. The hidden layer is initially set to 20 hidden neurons. The hidden layer uses sigmoid as the transfer function.

Step 3: Parameter initialization

We set the regularization coefficient, λ , and randomly initialize, w and b , so that their mean value is 0 and the variance is 1. The range is $[-1, 1]$.

Step 4: Training RVFLNN

The training data are input into the RVFLNN for training to get β . Then the predicted data can be obtained with β .

Step 5: Training error, validation error evaluation and parameters adjustment

The average relative error of training data is calculated to evaluate the model accuracy. We adjust the number of nodes in the hidden layer by comparing the training error and the validation error. When the training error keeps decreasing and the validation error no longer decreases, but increases, that is, before the overfitting, the network learning is stopped and the number of hidden layer nodes at this time is determined. Then minimize the training error by changing the regularization coefficient and the range of w and b . In the meantime, we stop the algorithm.

Step 6: Test RVFLNN performance

The test data are used to evaluate the model performance based on the trained RVFLNN.

3.4 Results and Analysis

3.4.1 Effects of training parameters

With the RVFLNN, the predicted temperatures are closer to experimental temperatures by adjusting the number of hidden layer nodes, L , and the regularization coefficient, λ . In this paper, the model accuracy is evaluated by the average relative error, E . It can be calculated with Eq.(9):

$$E = \frac{1}{N} \sum_{i=1}^N \left| \frac{T_{sim,i} - T_{exp,i}}{T_{exp,i}} \right| \quad (9)$$

where $T_{exp,i}$ and $T_{sim,i}$ are the experimental data and prediction data, respectively; N is the total number of sampling points.

Table .1 Effects of different hidden layer nodes on model performance.

(a)S2

Node numbers	20	50	100	200	300	400	600	800	1000
$E_{train} \times 10^{-3}$	3.687	3.435	3.404	3.438	3.333	3.284	3.271	3.235	3.224
$E_{validation} \times 10^{-3}$	4.532	4.201	4.144	4.119	4.067	3.991	3.972	3.910	3.941

(b)S3

Node numbers	20	50	100	200	300	400	600	800	1000
$E_{train} \times 10^{-3}$	4.657	4.391	4.294	4.162	4.126	4.122	3.958	3.930	3.920
$E_{validation} \times 10^{-3}$	6.011	5.807	5.490	5.452	5.528	5.613	5.487	5.502	5.494

(c)S4

Node numbers	20	50	100	200	300	400	600	800	1000
$E_{train} \times 10^{-3}$	3.229	2.866	2.791	2.720	2.695	2.660	2.629	2.600	2.585
$E_{validation} \times 10^{-3}$	6.880	6.760	6.714	6.824	6.773	6.846	6.763	6.821	6.773

E_{train} and $E_{validation}$ are the average relative errors of training data and validation data. After the initialization of RVFLNN parameters, the number of hidden layer nodes is adjusted. It can be seen from Table.1, when the number of hidden layer nodes gradually increases from 20 to 1000, the training error continuously decreases. However, when the hidden layer nodes separately reach about 800, 200 and 100, the test error will not approximately change or even begins to increase or fluctuate. Therefore, we can draw a conclusion that the generalization effect of RVFLNN will be good when the number of hidden layer nodes is 800, 200 and 100 for three different RVFLNN models, separately. At this moment, we determine the number of hidden layer nodes.

For the RVFLNN, after determining the hidden layer nodes, we adjust the regularization coefficients and the ranges of w and b . Taking RVFLNN model S3 as an example, we can observe from Table 2 that no matter what the range of w and b is, the validation error will reach the minimum when the regularization coefficient is about 0.5 or 1. Moreover, the range of w and b has no significant effect on the minimum error. In conclusion, the system performance will be better when the regularization coefficient is finally determined as 1 and the range of w and b is [-1, 1].

Table .2 Effects of different ranges of λ and ω , b on model performance.

λ	$\omega, b \in [-0.5, 0.5]$	$\omega, b \in [-1, 1]$	$\omega, b \in [-2, 2]$
	$E_{validation} \times 10^{-3}$	$E_{validation} \times 10^{-3}$	$E_{validation} \times 10^{-3}$
0.05	5.554	5.596	5.917
0.1	5.557	5.586	5.667

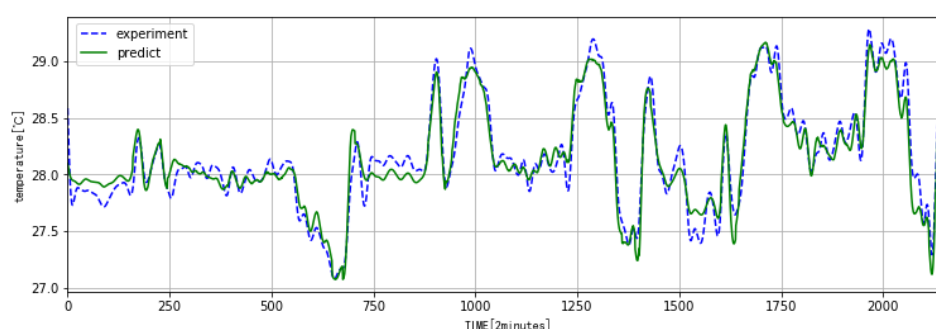
0.5	5.485	5.464	5.632
1	5.478	5.455	5.447
5	5.491	5.630	5.626
10	5.826	5.725	5.681
20	6.683	6.030	5.691

3.4.2. Prediction performance of thermal model based on RVFLNN

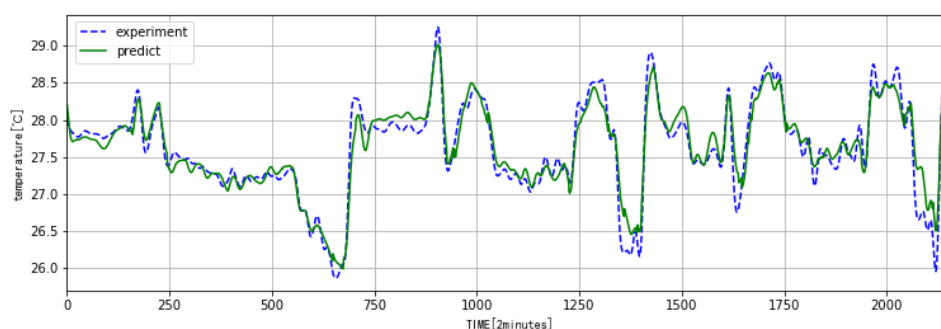
From the above analysis, the training parameters are finally determined, that is the number of hidden layer nodes is 400 and the range of w and b is $[-1, 1]$. Hence, the thermal model based on RVFLNN can be built with the above parameters. Fig. 6 gives the comparison results of prediction data with experimental data. Fig. 7 shows the relative error of prediction and experimental data. The relative error can be calculated with Eq.(10):

$$E_{relative} = \left| \frac{T_{sim,i} - T_{exp,i}}{T_{exp,i}} \right| \times 100\% \quad (10)$$

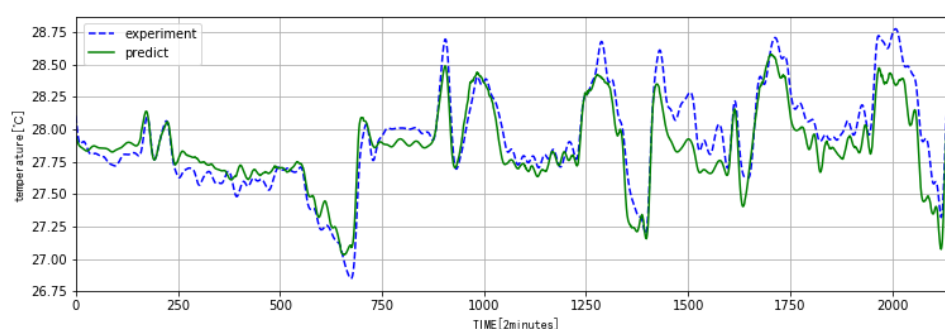
where $T_{exp,i}$ and $T_{sim,i}$ are the experimental data and prediction data.



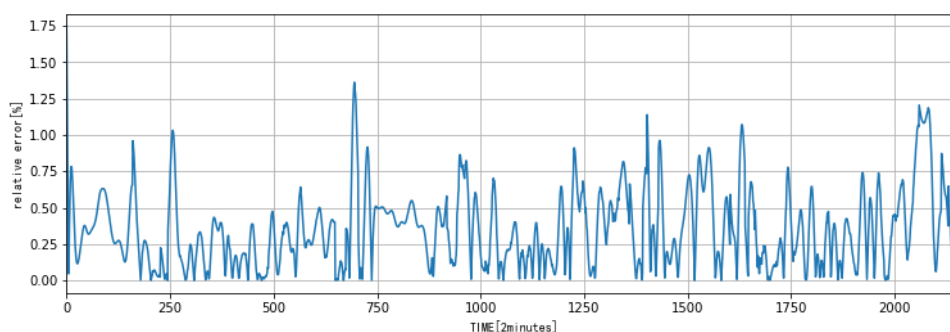
(a) S2



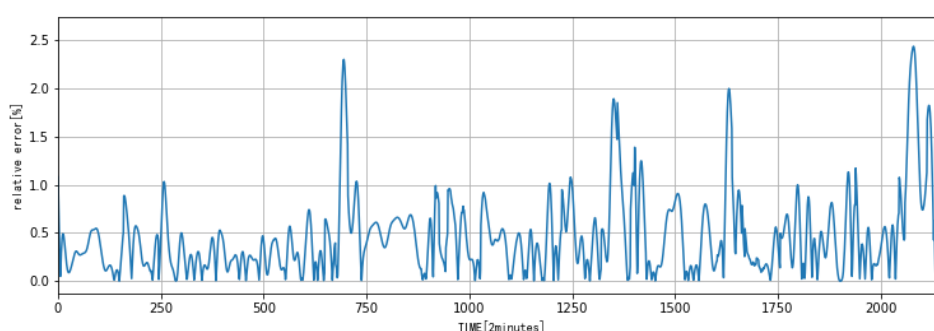
(b) S3



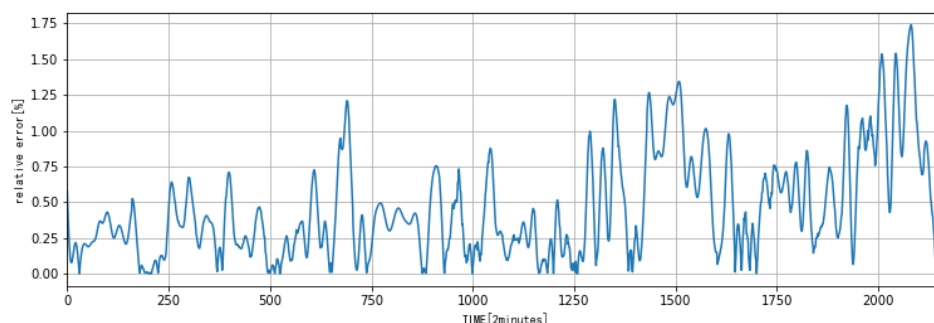
(c) S4

**Fig.6** comparison of predict data with experimental data.

(a) S2



(b) S3



(c) S4

Fig.7 relative error of prediction and experimental data.**Table .3** test error of three RVFLNN models

	S2	S3	S4
E_{test}	4.124	5.513	6.925


The following conclusions can be drawn from Fig. 6, Fig 7 and Table.3:




(1) The temperature change in the metro station is influenced by many factors and its change rule is relatively complicated. The presented model based on the RVFLNN can reveal this rule very well. Its fitting error and prediction error are very small.

(2) Comparison of the prediction data and experimental data shows that the maximum absolute error is about 0.4°C and the maximum relative error is about 2.5%.

(3) The test error can be just a little higher than the validation error in three different RVFLNN models. It can also be seen in Fig.6 and Fig.7.

The model accuracy has reached a good level and the presented modeling method can be used for the future temperature prediction in a metro station. 

4. Conclusion

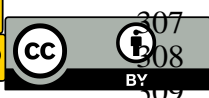
In this paper, a thermal environment modeling method based the RVFLNN is proposed for the metro station. By analyzing the interaction between the passenger flow, the metro arrival frequency and temperature inside the station, the thermal relationship of input variables and output variables for RVFLNN is carefully set up. The training time of the RVFLNN is very short, only about 0.002 seconds, which shows that the RVFLNN has a fast nonlinear modeling ability. It can accurately learn the relationship between the input and output variables of a given data set, and achieve relative high model accuracy. In model S2, the prediction error for the whole experimental conditions is within 0.25°C, and the relative error is kept within 1.4%, and the test error is within 4.124 . In model S3, the prediction error for the whole experimental conditions is within 0.5°C, and the relative error is kept about 2.5%, and the test error is within 5.513. In model S4, the prediction error for the whole experimental conditions is within 0.5°C, and the relative error is kept within 1.75%, and the test error is within 6.925. In conclusion, the model accuracy can be satisfied by using the RVFLNN. This study may have guide for the temperature prediction and control for the metro station. 

 **Acknowledgment:** This work was funded by the National Key R&D Program of China (2017YFB1201100)

References

1. Ma Zhanlong, Wang Gaowen Zhang Jian, Gu Yongqiang, Dai Lei, Simulation and forecast of the grinding temperature based on finite element and neural network, JOURNAL OF ELECTRONIC MEASUREMENT AND INSTRUMENT (2013)
2. Wu Baohai, Cui Di, He Xiaodong, Zhang Dinghua, Tang Kai, Cutting tool temperature prediction method using analytical model for end milling, Chinese Journal of Aeronautics (2016)
3. Jie Deng, Rongjiang Ma, Guofeng Yuan, Dynamic thermal performance prediction model for the flat-plate solar collectors based on the two-node lumped heat capacitance method, Solar Energy (2016)
4. R, Le Tellier, E. Skrzypek, L. Saas, on the treatment of plane fusion front in lumped parameter thermal models with convection, Applied Thermal Engineering (2017)
5. C.P. Underwood, An improved lumped parameter method for building thermal modeling, Energy and Buildings (2014)
6. A. Mezrhab, M. Bouzidi, computation of thermal comfort inside a passenger car compartment, Applied Thermal Engineering (2006)
7. Z. Tian, Ch. Qian, B. Gu, Electric vehicle air conditioning system performance prediction based on artificial neural network, Applied Thermal Engineering (2015)
8. Yasmine Korteby, Yassine Mahdi, Amel Azizou, Implementation of an artificial neural network as a PAT tool for the prediction of temperature distribution within a pharmaceutical fluidized bed granulator, European Journal of Pharmaceutical Sciences (2016)
9. Bamiji Z. Adewole, Artificial neural network prediction of exhaust emissions and flame temperature in LPG (liquefied petroleum gas) fueled low swirl burner, Energy (2013)
10. R. Dhanuskodi, R. Kaliappan, S. Suresh, Artificial Neural Network model for predicting wall temperature of supercritical boilers, Applied Thermal Engineering, 749-753 (2015)
11. Fuat Kara, Kubilay Aslantas, Adem Cicek, Prediction of cutting temperature in orthogonal machining of AISI 316L using artificial neural network, Applied Soft Computing, 64-74, (2016)
12. S.O. Starkov, Y.N. Lavrenkov, Prediction of the moderator temperature field in a heavy water reactor based on a cellular neural network, Nuclear Energy and Technology, 133-140, (2017)

13. Xiaojun Wang, Mingshuang You, Zhizhong Mao, Tree-Structure Ensemble General Regression Neural Networks applied to predict the molten steel temperature in Ladle Furnace, *Advanced Engineering Informatics* 368-375,(2016)
14. B.Igelnik, Y.-H.pao, S.LeClair, C.Y.Shen, The ensemble approach to neural-network learning and generalization, *IEEE Trans. Neural Netw.*10(1), 19-30, (1999)
15. C.R.Rao, S.K.Mitra, *Generalized Inverse of Matrices and Its Applications*, Wiley, New York,(1971)
16. Wang D, Alhamdoosh M, Evolutionary extreme learning machine ensembles with size control, *Neurocomputing* (2013)
17. Igelnik B, Pao Y H. Stochastic choice of basis functions in adaptive function approximation and the functional-link net[J]. *IEEE Transactions on Neural Networks*, 6(6):1320-9. (1995)
18. Simone Scardapane, Dianhui Wang, Massimo Panella, Aurelio Uncini, *Distributed learning for Random Vector Functional-Link networks*, *Information Sciences* Volume 301, 20 April 2015, Pages 271-284.
19. Yoh-Han Pao, Gwang-Hoon Park, Dejan J. Sobajic Learning and generalization characteristics of the random vector functional-link net, *Neurocomputing* Volume 6, Issue 2, April 1994, Pages 163-180.
20. Wang D, Alhamdoosh M. Evolutionary extreme learning machine ensembles with size control[J]. *Neurocomputing*, 2013, 102(102):98-110.
21. Alhamdoosh M, Wang D. Fast decorrelated neural network ensembles with random weights[J]. *Information Sciences*, 2014, 264(6):104-117.



© 2018 by the authors. Submitted for possible open access publication under the terms and conditions of the Creative Commons Attribution (CC BY) license (<http://creativecommons.org/licenses/by/4.0/>).